

# Fatigue testing of a NiTi rotary instrument. Part 1: strain–life relationship

G. S. P. Cheung<sup>1</sup> & B. W. Darvell<sup>2</sup>

<sup>1</sup>Family Dentistry & Endodontics; and <sup>2</sup>Dental Materials Science, Faculty of Dentistry, The University of Hong Kong, HKSAR, China

## Abstract

**Cheung GSP, Darvell BW.** Fatigue testing of a NiTi rotary instrument. Part 1: strain-life relationship. *International Endodontic Journal*, **40**, 612–618, 2007.

**Aim** To examine the fatigue behaviour using a strain-life approach, and to determine the effect of water on the fatigue life of a NiTi rotary instrument.

**Methodology** Instruments of one brand of NiTi engine-file (size 25, ProFile 0.04 and 0.06) were subjected to rotational bending either in air or under water, the number of revolutions to fracture ( $N_f$ ) being recorded using an optical counter and an electronic break-detection circuit. The effective surface strain amplitude ( $\epsilon_a$ ) for each specimen was determined from the curvature of the instrument (on a photograph) and the diameter of the fracture cross-section (from a scanning electron micrograph of the fracture surface). Strain was plotted against fatigue life and the low-cycle fatigue (LCF) region identified. Values were examined using two-way

analysis of variance for difference between various instrument–environment combinations.

**Results** A total of 212 instruments were tested. A strain-life relationship typical of metals was found.  $N_f$  declined with an inverse power function dependence on  $\epsilon_a$ . A fatigue limit was present at about 0.7% strain. The apparent fatigue-ductility exponent, a material constant for the LCF life of metals, was found to be between  $-0.45$  and  $-0.55$ . There was a significant effect of the environmental condition on the LCF life, water being more detrimental than air.

**Conclusions** The fatigue behaviour of NiTi rotary instrument is typical of most metals, provided that the analysis is based on the surface strain amplitude, and showed a high-cycle and a LCF region. The LCF life is adversely affected by water.

**Keywords:** breakage, failure, fracture, low-cycle fatigue, nickel–titanium, root canal instrument.

Received 17 November 2006; accepted 5 February 2007

## Introduction

A recent survey of 7159 NiTi rotary instruments discarded by 14 endodontic clinics in four countries has indicated that 5% of the instruments had fractured; 1.5% were classified as ‘torsional’ and 3.5% as ‘flexural (fatigue)’ failures (Parashos *et al.* 2004). That is, some 70% of fractures were attributable to ‘flexural fatigue’. The classification was based on the description of Sattapan *et al.* (2000), who reported some 44% of

breakages being attributable to flexural fatigue. Although such a classification did not take into account the fracture mechanism (Cheung *et al.* 2005, Shen *et al.* 2006), fatigue is undoubtedly an important mechanism leading to instrument failure in use.

The vast majority of root canals are curved. An engine-file rotating in the confines of such a curvature is subject to rotational bending which, indeed, is a widely used fatigue test for structural metallic materials (Collins 1993) – the fatigue life of most metallic materials in the low-cycle fatigue (LCF) region is a function of the strain amplitude (Suresh 1998). Although this test method has also been adopted for examining the fatigue behaviour of NiTi rotary instruments (Pruett *et al.* 1997, Haikel *et al.* 1999, Yared *et al.* 1999, 2001 Li *et al.* 2002, Peters *et al.* 2002, Fife

Correspondence: Dr Gary S.P. Cheung, Family Dentistry & Endodontics, Faculty of Dentistry, The University of Hong Kong, Floor 3A, Prince Philip Dental Hospital, 34 Hospital Road, Hong Kong (Tel.: +852 2859 0288; fax: +852 2559 9013; e-mail: spcheung@hku.hk).

*et al.* 2004, Ullmann & Peters 2005, Viana *et al.* 2006), little attention has been given to the magnitude of strain (i.e. deformation per unit length) imposed on the rotating instrument. In only one study (Bahia & Buono 2005), was there an attempt to estimate the strain from the advertised dimension of the instrument, but at the mean length averaged across all specimens; such a calculation has considerable error from the point of view of individual specimens. To date, nearly all other reports have merely described how the radius of curvature and the dimensions (size and taper) of an instrument influence the fatigue life of NiTi engine-files without really defining the relationships thereof. This has arisen from the lack of attention given to the magnitude of strain on the instrument during the test. Furthermore, the effect of an aqueous environment on the fatigue behaviour has never been reported in the dental literature. Thus, the purposes of this investigation were to: (i) examine the fatigue behaviour using a strain-life approach and (ii) determine the effect of water on the fatigue life of a NiTi rotary instrument. The null hypothesis was that NiTi engine-files of different dimensions have a similar fatigue life in air and in water.

## Materials and methods

A machine which comprised a reduction handpiece (E16R; NSK, Tokyo, Japan) mounted rigidly on a stainless steel frame was constructed. The handpiece

was driven by an electric motor (Tecnika, ATR, Milan, Italy) at maximum torque setting and a rate of 250 rpm. A slotted disk was mounted on a latch-grip extension to allow registration of the number of revolutions, to the nearest one-tenth of a revolution, by an optical sensor (Opto-Switch 303-1192; RS Components, NT, Hong Kong). The revolution counter was set to run automatically once the motor began to rotate; the accuracy of the reading was checked with a stroboscope (Strobatac 1538-A; General Radio, Concord, MA, USA). An electronic break-detection circuit, which triggered the optical counter and a digital timer, was used to detect instrument fracture. Three smooth cylindrical pins of 2-mm diameter from a high-hardness stainless steel were set in acrylic shims, which themselves were adjustable in the horizontal direction (Fig. 1); the position of the pins determined the curvature of the instrument whilst in motion. A small V-shaped groove was prepared on the lowest pin to maintain the position of the tip of the instrument during rotation.

One brand of NiTi rotary instrument (size 25, ProFile, 0.04 and 0.06 taper; Dentsply Maillefer, Ballaigues, Switzerland), denoted below as PF04 and PF06, respectively, was tested. Each instrument in turn was mounted in the handpiece and lowered to a position where its tip was level with the bottom edge of the lowest pin. The shims, and hence the pins, were then displaced horizontally such that the shaft of the instrument remained vertical above the top pin and the

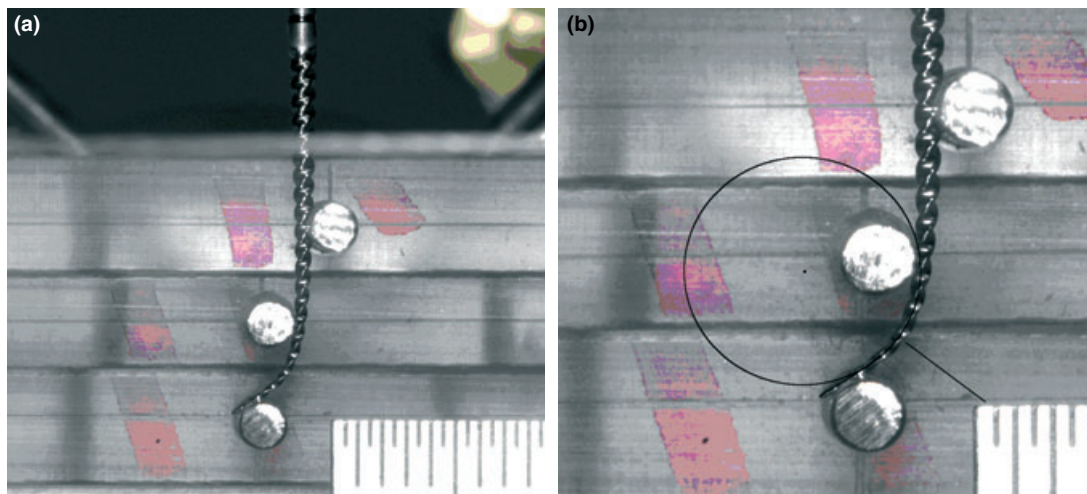


**Figure 1** (a) PF06 instrument constrained into a curvature by three rigid pins set in acrylic shims. (b) Determination of the curvature by best-fitting a circle to the instrument's central axis at site where breakage occurred (indicated by a radial line referring to the length of the fracture fragment).

bend occurred between the middle and the lowest one (Fig. 1). The instrument was allowed to rotate briefly, for no more than 2 s, to ensure that it was centred and did not slip sideways on the pins. A digital photograph at a fixed distance and magnification was taken at this stage. Then, the test was run at a rotation rate of 250 rpm until the instrument fractured; the total number of revolutions to failure  $N_f$  was recorded. The fragment was collected, its length measured and then mounted so that its long axis was normal to the microscope stage for examination of the fracture surface under SEM (either Cambridge Stereoscan 440, Cambridge, UK or XL-30cp, Phillips, Eindhoven, The Netherlands).

For each set of pin positions, the test was repeated twice wherever possible (except for those subjected to very low strain and with an extended life of over  $10^5$  cycles). To examine the effect of strain amplitude, a minimum of 15 sets of pin positions were used for each group. The tests were first done in air at an ambient temperature of  $23 \pm 2$  °C,  $65 \pm 10\%$  relative humidity. The experiment was then repeated by immersing the shims, pins and the rotating instrument in deionized water throughout, the water bath being maintained at the same temperature.

### Analysis of photographic images

The curvature for each instrument was determined on the digital photograph on a computer using image analyser software (ImageJ 1.34n, NIH, Bethesda, MD, USA). This was done by first transferring the corresponding breakage position, from the measured length of the fractured fragment, onto the photographic image (and drawing a radial line to indicate that position) and then best-fitting a circle to coincide without crossing the mid-line of the curved instrument for as great a distance as possible (Fig. 1b). All photographs were traced, blinded (i.e. without reference to test details) and the radius of the fitted circle taken as representing the curvature  $R_c$ , during rotational bending, leading to fatigue failure of that instrument.

### SEM images and data analysis

On each digitized scanning electron micrograph, a circle was fitted to encircle the fracture surface using the same software (ImageJ 1.34n). The diameter of the instrument at break  $d$  was determined for calculating the maximum surface strain amplitude  $\varepsilon_a$  (assuming

the instrument to be circular in cross-section) (Wick *et al.* 1995):

$$\varepsilon_a = \frac{d}{2R_c} \quad (1)$$

Strain was plotted against fatigue life, on logarithmic scales, in software (SigmaPlot 9.0, Systat Software, Richmond, CA, USA). The shape of the plot was evaluated to estimate the transition from low-cycle to high-cycle fatigue. A regression line was then fitted to the LCF region, in software (SigmaPlot 9.0), for determining the apparent fatigue-ductility exponent,  $c$  (that is, the slope of the line and which is a material constant in the Coffin-Manson equation for LCF life of metals; Collins 1993, ASM International 1996), for each group of instruments in the two environmental conditions. The values were analysed using two-way analysis of variance (ANOVA) in software (SPSS for Windows 11.0, SPSS, Chicago, IL, USA), at  $\alpha = 0.05$ , to examine for any difference as well as interaction between instrument dimension and environmental condition.

## Results

A total of 111 PF04 and 101 PF06 instruments were tested at various curvatures in air and water (Table 1). Overall, there was a general trend of a rapidly declining life at high strain amplitudes, which rate then decreased at about 1.5% strain (Fig. 2). A true fatigue limit, at about 0.7% strain, seemed to be present, some  $2 \times 10^6$  revolutions being survived by an instrument without breakage (indeed, it outlasted the electric motor during the test). Several runs were also

**Table 1** Number of instruments tested and the range of cycles to failure

Group	Batch numbers <sup>a</sup>	No. of instruments tested	Maximum surface strain amplitude (%)	No. of revolutions to failure <sup>b</sup>
PF04				
air	5571110, 4238920	52	9.11–0.74	193–( $10^5$ )
water	3701510	59	8.67–0.76	151–( $10^6$ )
PF06				
air	3635500, 2378190	54	8.57–0.69	107–( $10^5$ )
water	5154060	47	9.97–0.85	134–56938

<sup>a</sup>More than one batch were used in some groups because there were insufficient numbers to complete the test.

<sup>b</sup>Number in brackets indicated that the instrument did not break when the test was interrupted.

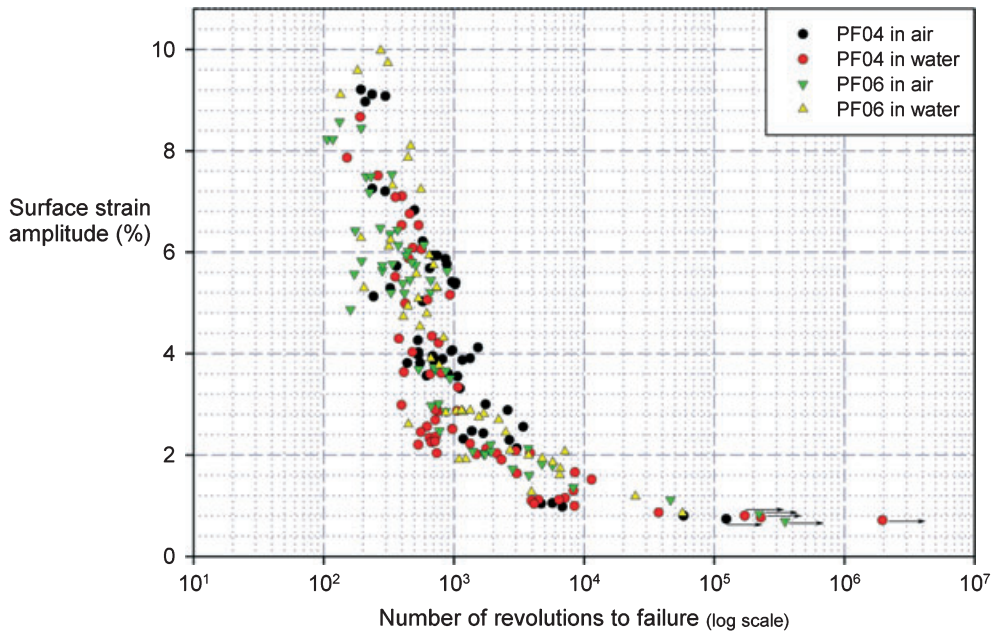


**Figure 2** Relationship between the maximum surface strain amplitude and the fatigue life of PF04 and PF06 instruments tested in air and water. Symbols with an arrow indicate those which did not break when the test was abandoned.

interrupted after some  $10^5$ – $10^6$  cycles also because of breakdown of the motor.

A transition in the slope of the plot (Fig. 2) was noted at about 4000 cycles. The relationship between the strain amplitude and fatigue life in the LCF region ( $N_f < 4000$  cycles) was individually plotted for each instrument–environment combination (not shown), for which a regression line could be fitted ( $0.63 < r^2 < 0.80$ ;  $P < 0.001$ ). The fatigue-ductility exponent  $c$  was determined from the slope of the line, which value ranged from  $-0.45$  to  $-0.55$  for the various combinations (Table 2); there was a significant difference between groups (two-way ANOVA,  $P < 0.05$ ). On the other hand, the value for PF04 in air did not differ from

that for PF06 in air, nor between the two instruments in water. Testing on the pooled data indicated a significant difference in the LCF behaviour between the two environmental conditions (one-way ANOVA,  $P < 0.05$ ) (Fig. 3). The value of  $c$  was  $-0.45$  ( $r^2 = 0.72$ ) and  $-0.55$  ( $r^2 = 0.66$ ) in air and under water, respectively.

Statistical testing was not done for the high-cycle fatigue lives (i.e.  $N_f > 4000$  cycles) in view of the very small number of results obtained for this region and that most breakages of NiTi instruments, as reported in the literature, fall in the LCF region.

**Discussion**

There are three basic types of fatigue test for various design philosophies: (i) the ‘stress-life’ approach for safe, durable parts designed for an extended working life, (ii) the ‘strain-life’ approach for a safe, finite but predictable life of parts that may be used at relatively high service loads and (iii) the ‘damage tolerant’ approach which allows for the estimation of the extent of crack growth in terms of the number of cycles before fracture may occur so that timely replacement of the parts may be planned (ASM International 1996, Suresh 1998). Studies have shown that NiTi alloys which undergo stress-induced martensitic (SIM) or

**Table 2** Apparent fatigue-ductility exponent derived from the LCF lives ( $N_f < 4000$  cycles) for various groups

Instrument	Immersion medium	N	<sup>a,b</sup> Fatigue-ductility exponent, $c$ ( $\pm$ SE)	Coefficient of determination
PF04	Air	47	$-0.452 \pm 0.048$	0.6647
	Water	47	$-0.553 \pm 0.063$	0.6296
PF06	Air	48	$-0.484 \pm 0.035$	0.8043
	Water	40	$-0.549 \pm 0.054$	0.7320

<sup>a</sup>The value of the slope of the regression line and the standard error were obtained in software (SigmaPlot 9.0).

<sup>b</sup>There is a significant difference in the slope of the fitted line between various instrument–immersion medium combinations (two-way ANOVA,  $P < 0.05$ ).

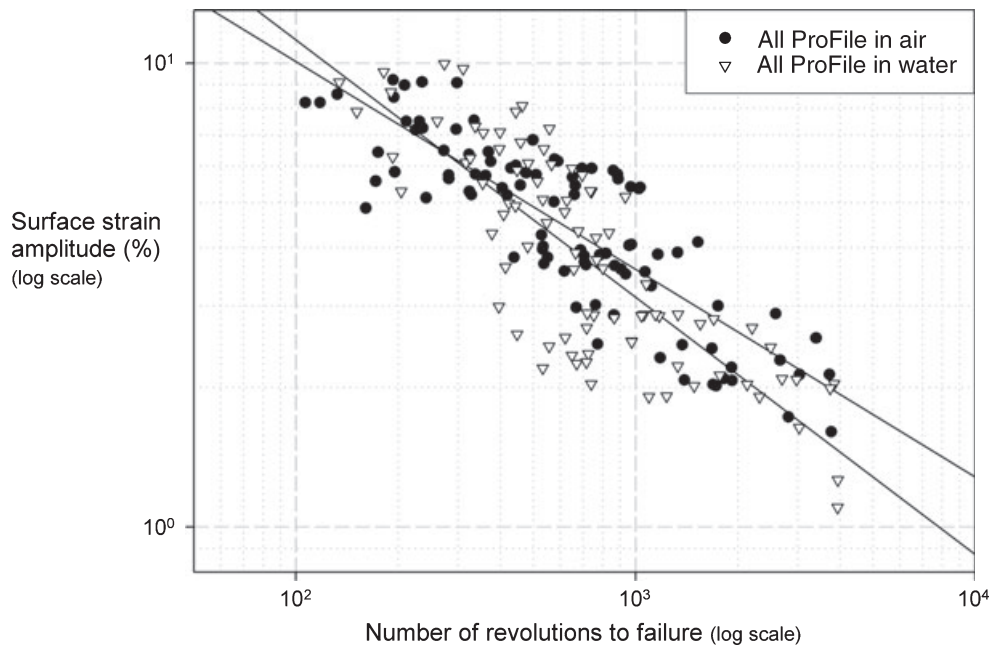


**Figure 3** Strain-life relationship (pooled data for PF04 and PF06) at the LCF region ( $N_f < 4000$  cycles) of ProFile instruments fatigued in air (A) and water (W). The value of the slope of the regression line (i.e. fatigue-ductility coefficient  $c$ ) was significantly different between the two environmental conditions (one-way ANOVA,  $P < 0.05$ ).

so-called 'superelastic' transformation during every load cycle are less tolerant of fatigue-crack growth; the crack propagation rate is greater in transforming than nontransforming NiTi (Dauskardt *et al.* 1989, McKelvey & Ritchie 1999). In other words, extending the cyclic stress or strain into or beyond the superelastic range (usually between 1% and 6% strain; Gallardo Fuentes *et al.* 2002) will lead to a decrease in the fatigue life of NiTi alloys. The critical stress for SIM transformation, which depends initially on the history of heat treatment and the amount of cold work of the material (Saburi 1989), changes as the material work-hardens upon repeated loading (Duerig & Pelton 1994). This would render stress-based fatigue tests rather difficult to control. On the other hand, the strain-life approach simulates the clinical situation whereby instruments are confined to a certain curvature (in a curved root canal) whilst rotating, and therefore is considered an appropriate means for examining the fatigue behaviour of NiTi rotary files.

When the fatigue life of a NiTi rotary instrument is expressed as a function of the effective strain amplitude at the surface, a strain-life relationship, typical of all metal solids (i.e. with a low- and a high-cycle fatigue region), is obtained. The instrument in this study was constrained into a curvature using three stainless steel

pins. It has been reported in a three-point bending test of NiTi wires that such constraints will produce a curvature which is circular (Wick *et al.* 1995); although this cannot actually be true, the approximation is reasonable. In nearly all studies reported in the endodontic literature, the rotating instrument was either confined in a metal tube (Pruett *et al.* 1997, Yared *et al.* 1999, 2001) or in a grooved block-and-rod assembly (Haikel *et al.* 1999, Peters *et al.* 2002, Fife *et al.* 2004, Ullmann & Peters 2005, Viana *et al.* 2006); there has been no mention of the 'fit' of the instrument in the tube or groove. As the instrument is likely to be fitting loosely (to reduce friction or avoid being jammed), the description of the radius of curvature in those studies is likely to be overstated; that is, the file was actually bent less severely than reported. That would explain the wide variation in the reported fatigue life. The large scatter generally encountered in various forms of fatigue tests (Weibull 1961) would add to the variation in the result. In this present study, the strain amplitude was calculated from the radius of curvature and the 'postmortem' diameter of the broken fragment with the intention of more accurately estimating the imposed strain on each instrument at the point of failure. This approach is considered preferable to simple calculation from the fragment length and to allow for

variation in both nominal size and taper of the instrument because of manufacturing tolerances.

An apparent fatigue-ductility exponent  $c$  is determined from the slope of the plot of the strain amplitude versus the fatigue life in the LCF region on logarithmic scales (Collins 1993, ASM International 1996). Although the NiTi rotary instrument used in this study does not conform to the shape and dimension for the 'usual' fatigue test in the engineering context, the value of  $c$  (between  $-0.45$  and  $-0.55$ ) is in keeping with the general value reported for NiTi alloys (Tolomeo *et al.* 2001, Pelton *et al.* 2004). Thus, the NiTi rotary instruments generally behaved in the same manner as superelastic NiTi wires if the analysis is based on the magnitude of surface strain, instead of merely the radius of curvature as is commonly reported in the literature. Indeed, a fatigue limit at about 0.7% strain has been reported for cylindrical NiTi wires (Tobushi *et al.* 1997). This is not surprising because the manufacturing process merely imparts a shape to the instrument; none of these commercial products have apparently received any post-manufacture heat or surface treatment, which treatments would influence the fatigue behaviour of NiTi alloys by altering the bulk material properties (heat treatment) and susceptibility to fatigue-crack initiation (surface condition), respectively.

The results here indicated that the fatigue lives of PF04 and PF06 cycled either in air, or under water, were comparable. That is, the dimension (taper) of the instrument did not influence the fatigue life, provided that the analysis was based on the surface strain amplitude. Notice that for PF04 cycled with the same curvature and strain amplitude as a PF06 instrument, the fragment length would be longer than (and hence the effective diameter at break is similar to) that for PF06, which relationship is given in Equation (1). Indeed, it was noted that the location of the maximum curvature, i.e. where breakage occurred, was situated closer to the tip of a PF06 than for a PF04 instrument when the two instruments were similarly displaced.

Some effect of water on the LCF life was discernible – those fatigued in water gave a greater (absolute) value of the apparent fatigue-ductility exponent than in air. This is in contrast to reports of testing on smooth cylindrical wires, which suggested a similar behaviour (Tobushi *et al.* 2000). The various cross-sectional forms and the presence of machining grooves (obvious in most NiTi rotary instruments; see scanning electron micrographs of the instrument surface in Alapati *et al.* 2003, Peng *et al.* 2005 and Alexandrou *et al.* 2006) might have contributed to the difference. Besides, water

seemed to have some effect on the crack initiation process in the material (Cheung & Darvell 2007). Clinically, root canal treatment is invariably carried out in conjunction with copious irrigation. The irrigant solution is injected and remains in the root canal, whilst the instrument is used to prepare the root canal wall (i.e. cutting dentine). As the fatigue behaviour of NiTi rotary instruments in air differs from that in water, it is paramount that testing of their fatigue behaviour is carried out in at least an aqueous environment, rather than in air, to simulate the clinical situation more closely.

## Conclusions

The fatigue behaviour of NiTi rotary instruments is typical of most metallic materials, demonstrating a low-cycle and a high-cycle fatigue region, provided that the analysis is based on the surface strain imposed on the instrument. The LCF life of NiTi engine-files subjected to rotational bending is adversely affected by water.

## Acknowledgements

The following people are gratefully acknowledged for their assistance in this study: Mr Tony Yuen and Paul Lee of the Dental Materials Science Laboratory of the Faculty of Dentistry, The University of Hong Kong (HKU), for building the fatigue-testing machine; Mr Simon Lee of the Oral Bioscience Laboratory of the Faculty of Dentistry and Ms Amy Wong of the Electron Microscope Unit, HKU, for their technical assistance with the SEMs; Dr May Wong, Assistance Professor of the Faculty of Dentistry, HKU, for statistical analysis; and Dr Y. Shen, Associate Professor of the Department of Operative Dentistry and Endodontics, Stomatological School and Hospital, Wuhan University, Wuhan, China, for participation in the experimental work.

## References

- Alapati SB, Brantley WA, Svec TA, Powers JM, Mitchell JC (2003) Scanning electron microscope observations of new and used nickel-titanium rotary files. *Journal of Endodontics* **29**, 667–9.
- Alexandrou G, Chrissafis K, Vasiliadis L, Pavlidou E, Polychroniadis EK (2006) Effect of heat sterilization on surface characteristics and microstructure of Mani NRT rotary nickel-titanium instruments. *International Endodontic Journal* **39**, 770–8.

- ASM International (1996) *ASM Handbook, vol. 19: Fatigue and Fracture*. Materials Park, OH: ASM International.
- Bahia MG, Buono VT (2005) Decrease in the fatigue resistance of nickel-titanium rotary instruments after clinical use in curved root canals. *Oral Surgery Oral Medicine Oral Pathology Oral Radiology and Endodontics* **100**, 249–55.
- Cheung GSP, Darvell BW (2007) Fatigue testing of a NiTi rotary instrument. Part 2: fractographic analysis. *International Endodontic Journal*, in press. doi: 10.1111/j.1365-2591.2007.01256.x
- Cheung GSP, Peng B, Bian Z, Shen Y, Darvell BW (2005) Defects in ProTaper S1 instruments after clinical use: fractographic examination. *International Endodontic Journal* **38**, 802–9.
- Collins JA (1993) *Failure of Materials in Mechanical Design: Analysis, Prediction, Prevention*. New York, NY: John, Wiley & Sons.
- Dauskardt RH, Duerig TW, Ritchie RO (1989) Effects of *in situ* phase transformation on fatigue-crack propagation in titanium-nickel shape-memory alloys. In: *Proceedings of the MRS International Meeting on Advanced Materials* **9**, 243–9.
- Duerig TW, Pelton AR (1994) Ti-Ni shape memory alloys. In: Boyer R, Welsch G, Collings EW, eds. *Materials Properties Handbook: Titanium Alloys*. Materials Park, OH: ASM International, pp. 1035–48.
- Fife D, Gambarini G, Britto L Jr (2004) Cyclic fatigue testing of ProTaper NiTi rotary instruments after clinical use. *Oral Surgery Oral Medicine Oral Pathology Oral Radiology and Endodontics* **97**, 251–6.
- Gallardo Fuentes JM, Gümpel P, Strittmatter J (2002) Phase change behavior of nitinol shape memory alloys. *Advanced Engineering Materials* **4**, 437–51.
- Haïkel Y, Serfaty R, Bateman G, Senger B, Allemann C (1999) Dynamic and cyclic fatigue of engine-driven rotary nickel-titanium endodontic instruments. *Journal of Endodontics* **25**, 434–40.
- Li U-M, Lee B-S, Shih C-T, Lan W-H, Lin C-P (2002) Cyclic fatigue of endodontic nickel titanium rotary instruments: static and dynamic tests. *Journal of Endodontics* **28**, 448–51.
- McKelvey AL, Ritchie RO (1999) Fatigue-crack propagation in nitinol, a shape-memory and superelastic endovascular stent material. *Journal of Biomedical Materials Research* **47**, 301–8.
- Parashos P, Gordon I, Messer HH (2004) Factors influencing defects of rotary nickel-titanium endodontic instruments after clinical use. *Journal of Endodontics* **30**, 722–5.
- Pelton AR, Gong X-Y, Duerig T (2004) Fatigue testing of diamond-shaped specimens. In: *SMST-2003: Proceedings of the International Conference on Shape Memory and Superelastic Technologies*. 293–302.
- Peng B, Shen Y, Cheung GSP, Xia TJ (2005) Defects in ProTaper S1 instruments after clinical use: longitudinal examination. *International Endodontic Journal* **38**, 550–7.
- Peters OA, Kappeler S, Bucher W, Barbakow F (2002) Engine-driven preparation of curved root canals: measuring cyclic fatigue and other physical parameters. *Australian Endodontic Journal* **28**, 11–7.
- Pruett JP, Clement DJ, Carnes DL Jr (1997) Cyclic fatigue testing of nickel-titanium endodontic instruments. *Journal of Endodontics* **23**, 77–85.
- Saburi T (1989) Structure and mechanical behavior of Ti-Ni shape memory alloys. In: *Proceedings of the MRS International Meeting on Advanced Materials, Shape Memory Materials* **9**, 77–91.
- Sattapan B, Nervo GJ, Palamara JEA, Messer HH (2000) Defects in rotary nickel-titanium files after clinical use. *Journal of Endodontics* **26**, 161–5.
- Shen Y, Cheung GS, Bian Z, Peng B (2006) Comparison of defects in ProFile and ProTaper systems after clinical use. *Journal of Endodontics* **32**, 61–5.
- Suresh S (1998) *Fatigue of Materials, 2nd edn*. Cambridge, UK: Cambridge University Press.
- Tobushi H, Hachisuka T, Yamada S, Lin P-H (1997) Rotating-bending fatigue of a TiNi shape-memory alloy wire. *Mechanics of Materials* **26**, 35–42.
- Tobushi H, Nakahara T, Shimeno Y, Hashimoto T (2000) Low-cycle fatigue of TiNi shape memory alloy and formulation of fatigue life. *Journal of Engineering Materials and Technology* **122**, 186–91.
- Tolomeo D, Davidson S, Santinoranont M (2001) Cyclic properties of superelastic nitinol: design implications. In: *SMST-2000: Proceedings of the International Conference on Shape Memory and Superelastic Technologies*, 471–6.
- Ullmann CJ, Peters OA (2005) Effect of cyclic fatigue on static fracture loads in ProTaper nickel-titanium rotary instruments. *Journal of Endodontics* **31**, 183–6.
- Viana ACD, Gonzalez BM, Buono VTL, Bahia MGA (2006) Influence of sterilization on mechanical properties and fatigue resistance of nickel-titanium rotary endodontic instruments. *International Endodontic Journal* **39**, 709–715.
- Weibull W (1961) *Fatigue Testing and Analysis of Results*. Oxford: Pergamon Press.
- Wick A, Vöhringer O, Pelton AR (1995) The bending behavior of NiTi. *Journal de Physique IV, Colloque C8 (ICOMAT-95)* **5**, 789–94.
- Yared GM, Bou Dagher FE, Machtou P (1999) Cyclic fatigue of ProFile rotary instruments after simulated clinical use. *International Endodontic Journal* **32**, 115–9.
- Yared GM, Bou Dagher FE, Machtou P (2001) Failure of ProFile instruments used with high and low torque motors. *International Endodontic Journal* **34**, 471–5.

This document is a scanned copy of a printed document. No warranty is given about the accuracy of the copy. Users should refer to the original published version of the material.